Journal of Ophthalmology and Ophthalmic Surgery

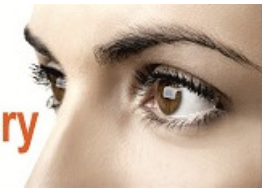

Research Article

Transducer Selection for In Vivo Ultrasonic Retinal Stimulation: A Porcine Eye Model Study

Jun Zhang[5], Yi Zhang[1,2], Juan-juan Gu[4], Yun Jing[4], Ruimin Chen[3], Mark S. Humayun[1,2,3], K. Kirk Shung[3], Andrew C. Weitz[1,2,3]* and Qifa Zhou[1,2,3]*

[1]USC Roski Eye Institute, University of Southern California, USA
[2]USC Institute for Biomedical Therapeutics, University of Southern California, USA
[3]Department of Biomedical Engineering, University of Southern California, USA
[4]Department of Mechanical and Aerospace Engineering, North Carolina State University, USA
[5]School of Power and Mechanical Engineering, Wuhan University, China

***Corresponding Author:** Dr. Andrew C. Weitz, Department of Ophthalmology, University of Southern California, USA; Tel: 323-865-0648; Fax: 323-865-0858; E-mail: aweitz@usc.edu

Dr. Qifa Zhou, Department of Ophthalmology and Department of Biomedical Engineering, University of Southern California, USA; Tel: 626-380-5675; Fax: 213-821-3897; E-mail: qifazhou@usc.edu

Published: October 10, 2016

Abstract:

Purpose: The aim of this study was to measure the frequency shift and attenuation of ultrasound propagation in the eye, in order to select an optimal frequency for ultrasonic retinal stimulation.

Methods and Materials: Transducers of different frequencies (3.5-MHz, 20-MHz, and 40-MHz) were used to measure the intensity attenuation coefficient and center frequency shift in enucleated porcine eyes. Numerical modeling of acoustic fields in an intact eye was used to explain the center frequency shift. Three types of porcine eye samples were made for comparing attenuation coefficients in dissected and intact eyes. A comparison of focused and planar transducers was also provided.

Result: 3.5-MHz ultrasound propagates through the eye with no significant frequency shift. At 20- and 40-MHz, however, the center frequency of the signal shifts to less than 15-MHz. The overall attenuation coefficients of the porcine eye are 0.13-dB/cm, 1.43-dB/cm, and 2.15-dB/cm at 3.5-MHz, 20-MHz, and 40-MHz respectively, which correspond to intensity losses of 51.25%, 96.31%, and 99.93% for an eye with a thickness of 24-mm. The attenuation coefficients of the dissected and intact eyes are within the same margin of error. There is no significant difference between the measurement results from the two types of transducers (focused and planar).

Conclusion: This study revealed that significant central frequency shifts and attenuation occurs when high-frequency ultrasonic transducers are used for in vivo retinal stimulation.

Keywords:
Attenuation; Central Frequency Shift; Intensity Loss; Retinal Stimulation; Ultrasound

Introduction: Inner retinal neurons remain largely functional during the progression of retinal degenerative diseases, which are a leading cause of incurable blindness [1]. Retinal prostheses that electrically stimulate surviving retinal neurons have demonstrated safety and efficacy in restoring artificial vision to patients blinded by these diseases [2,3]. Retinal prostheses require invasive surgeries and have inherent problems including long-term stability of the interface between the electrical components and retinal tissue [2]. Furthermore, image resolution is limited by the dimensions and quantity of the elements in the stimulating electrode array. An alternative approach to restoring vision to patients with retinal degenerative diseases is direct optical stimulation of retinal neurons using optogenetic probes. If validated clinically, this approach could offer single cell resolution but also requires injection of virus and carries the risk of immune reactions [3]. Hence, a minimally or non-invasive approach to restoring vision would be highly beneficial.

Ultrasound promises to be a useful, noninvasive tool for neural circuit research and neuromodulation [4]. Tufail et al. used transcranial pulsed ultrasound to stimulate intact mouse brain circuits and were able to evoke motor behaviors [5]. Legon et al. used transcranial focused ultrasound to modulate human cortical function [6]. Naor et al. explored the feasibility of using ultrasound to stimulate the retina as an alternative to microelectrode-based implants for artificial vision [7]. Recently, Menz et al. used high-frequency ultrasound to demonstrate spatially localized neural activation of *ex vivo* retina [8]. Although these studies have experimentally validated the feasibility of using ultrasound to elicit neuronal activity, many questions about the technological framework remain unsolved. One factor that must be considered is the correlation between ultrasound transducer parameters and the anatomy of the eye. For *in vivo* ultrasonic stimulation of retina, attenuation, and center frequency shift can occur when ultrasound waves penetrate the intact eyeball - a multilayered medium with curved interfaces. Accurate measurement of ultrasonic propagation properties in intact eyes is critically important for selection of the ultrasonic parameters used for retinal stimulation.

Previous work has focused on measuring the attenuation of each layer of the eyeball. Chivers et al. used a 10-MHz transducer to measure the attenuation of individual layers of human eyes, in order to validate their eye model based on ray tracing [9]. Korte et al. used a 20-MHz transducer to measure the frequency-dependent attenuation of dissected human and porcine eye tissues [10]. Ye et al. used a 60-MHz transducer to measure the ultrasonic properties of the human sclera, cornea, ciliary body, and iris [11]. In each of these studies, the lens proved to be responsible for the majority of acoustic attenuation. Various papers described the relationship between lens hardness and attenuation at different frequencies [12-16]. However, available acoustic data for the eyeball are limited due to the attenuation experiments being carried out on individual thin film eye tissue samples and the use of inconsistent measurement methods [10,11]. The acoustic attenuation of the intact eye was numerically calculated based on reported values of attenuation in isolated eye tissues [7]. Data for the eyeball are insufficient and inaccurate without considering the whole eye globe anatomy. Systematic measurement of ultrasonic attenuation and center frequency shift caused by attenuation of the high-frequency band in ocular tissues is still needed.

Ultrasound at a frequency lower than 20-MHz can undoubtedly reach the retina, as evidenced by the common practice of imaging the posterior segment of the eye in this frequency range [17-22]. However, frequencies higher than 20-MHz have been merely used for ultrasonic imaging of the anterior segment, instead of the posterior segment [23-26]. Unlike imaging applications, which are based on the pulse-echo mode, ultrasound for retinal stimulation needs only one-way propagation; therefore, higher frequency transducers may be suitable. Furthermore, there is a positive correlation between transducer frequency and the spatial resolution that can be achieved.

In this study, we used 5 transducers of different frequencies (3.5-MHz, 20-MHz, and 40-MHz; planar and focused) to measure the intensity attenuation coefficient of enucleated intact porcine eyes. Porcine eyes have been experimentally shown to serve as an animal model for studying ultrasound properties of the human eyes [10]. The attenuation coefficients and center frequency shift at each frequency are discussed and explained by numerical modeling of acoustic fields in an intact eye. The experimental results of dissected and intact samples are compared. A comparison of focused and planar transducers is also provided.

Materials and Methods:

Sample preparation: Fresh porcine eyes were purchased from a slaughterhouse. The extraocular muscles were cleared using a surgical knife. Three types of samples were prepared: The first was the intact eye, which was used for measuring the overall attenuation coefficient. The second was the eyeball with a hole made through the retina, choroid, and sclera, in order to measure the ultrasound intensity reaching the retina. The last was the eyeball with a layer of parylene covering the hole to prevent the vitreous body from flowing out. The thickness of the eyeball was measured by a Vernier caliper and ranged from 21-mm to 25-mm. The eye samples were placed in a holder with a hole in the center. The diameter of the hole was 12-mm, which was large enough for the ultrasonic beam to pass through. A solution with 5% gelatin was used to affix the eyeball.

Transducers: Five transducers were used in the experiment. The transducer with 3.5-MHz frequency was acquired from GE Measurement and Control, Ltd. The other 4 transducers were made in house. The element material was $LiNbO_3$ (Boston Piezo-Optics, Bellingham, MA).

The matching layer was made from Insulcast 501 composites consisting of Insulcure 9 (American Safety Technologies, Roseland, NJ) and silver particles (Aldrich Chemical Co., Milwaukee, WI, USA). The backing layer was made by E-Solder 3022 (VonRoll Isola, New Haven, CT). The thickness of the element was designed to be half of the sound wavelength in $LiNbO_3$. According to the results from the PiezoCAD simulation program (Sonic Concepts, Bothell, WA), the element diameters were designed to be 7.2-mm and 4-mm for the 20-MHz and 40-MHz transducers, respectively, in order to meet the electrical impedance matching conditions. The focal points were designed to be at the posterior segment of the eye. Focused transducers were made from curved elements. Planar element transducers with natural foci were also fabricated for comparison. The measured parameters of the transducers are listed in Table 1.

No.	Frequency (MHz)	Focal length (mm)	Bandwidth (%)	Diameter (mm)
1	3.5	12.7	19.74	6.35
2	21.09	unfocused	53.98	7.2
3	22.97	23.5	55.35	7.2
4	40.3	unfocused	62.77	4
5	40.5	23.5	71.7	4

Table 1: Parameters of the transducers

Experimental setup: The experimental setup is shown in Figure 1. The eyeball was affixed with 5% gelatin to a box holder with a circular window (12-mm diameter) for ultrasound transmission and reception. A quartz flat was placed under the holder to serve as a strong reflector, as there might not be any detectable echo reflected from the sclera. The distance between the eyeball and the quartz was 5-mm. The transducer was placed above the eyeball. Degassed saline solution was used to immerse the ultrasonic transducer, eyes, and quartz in all measurements. All measurements were performed at room temperature. A pulser/receiver (Panametrics 5900PR, Olympus, Waltham, MA) was used for transmitting and receiving ultrasound signals. The high pass and low pass cutoff frequencies were set at 1-MHz and 100-MHz, respectively. The pulse repetition frequency was 200-Hz. The energy was set to 1-μJ. The acoustic signal received from the reflector was acquired by a high-speed acquisition card (GAGE) with a sampling frequency of 1-GHz. A motorized translator was used to position the transducer. The average acoustic signals from 10 A-line scans were stored in a personal computer via custom software.

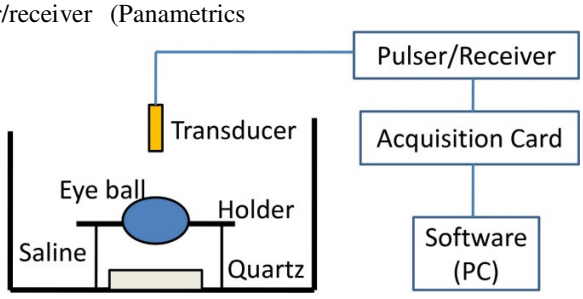

Figure 1: Schematic of the experimental setup

Data processing: The fast Fourier transform (FFT) was used to obtain the spectrum of the radio-frequency (RF) signal from the reflector. The thickness of the eye was calculated by the average velocity v and time interval $\Delta t=t_1 - t_2$. The average velocity v was calculated with the equation [27]

$$v = c\left(\frac{T_2 - T_1}{t_2 - t_1} + 1\right) \quad (1)$$

where T_1 and T_2 are the times of flight with and without the sample, and t_1 and t_2 are the times of flight from the top and bottom surfaces of the sample. The ultrasonic frequency-dependent attenuation coefficient α was calculated using the equation [27]

$$\alpha(f,z) = \frac{20(\lg P_0(f,z) - \lg P_1(f,z))}{2d(z)} \quad (2)$$

where P_0 and P_1 are the power spectrum of the echoes from the quartz in saline and the quartz with eyeball interposed, respectively. d is the thickness of the eye, which was calculated by the average velocity and time interval.

Attenuation in biological tissue can be described using a power law function

$$\alpha = \beta f^{n} \quad (3)$$

where α is the tissue attenuation in dB/cm, β is the coefficient of frequency-dependent attenuation (dB /cm/ MHz), and n is the power law exponent (usually between 0.9 and 1.4) [27].

Results and Discussion:

Central frequency shift: Center frequency is an important parameter for ultrasonic neuro-stimulation. The attenuation caused by absorption and scattering are highly frequency dependent. The bandwidths of the high-frequency transducers are larger than 50%, as shown in Table 1. If a transducer is driven by a pulse signal, the low-frequency portion of the signal will suffer less intensity attenuation. Consequently, a central frequency shift phenomenon will occur. Figures 2(a) and 2(b) show the spectrum of the signal transmitted and received from the quartz reflector using two focused transducers (3.5-MHz and 20-MHz). There was no obvious center frequency shift for the 3.5-MHz transducer, but a significant shift occurred for the 20-MHz transducer. Figure 2(c) shows that when 20 MHz ultrasound propagated through the eyeball, the measured central frequency ranged from 11.2-MHz to 14.7-MHz, with an average frequency of 12.7-MHz. For the 40-MHz transducer, the measured central frequency ranged from 10.0- to 17.5-MHz, with an average frequency of 13.3-MHz. Thus, the frequency shift became larger as the central frequency of the transducer increased. The central frequency of the ultrasound appeared to reach a saturation value (<15-MHz). For *in vivo* retina stimulation with pulsed signals, the central frequency of the ultrasound reaching the retina may be 10~20-MHz, regardless of how high the frequency is.

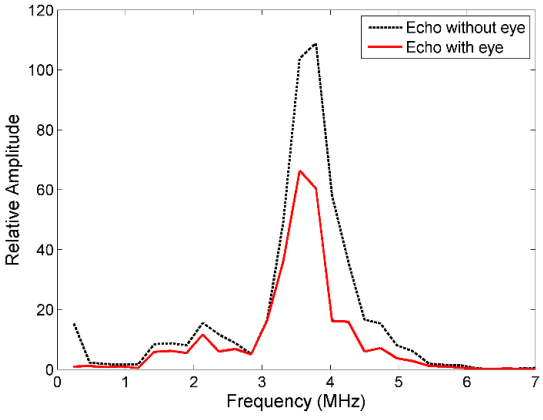

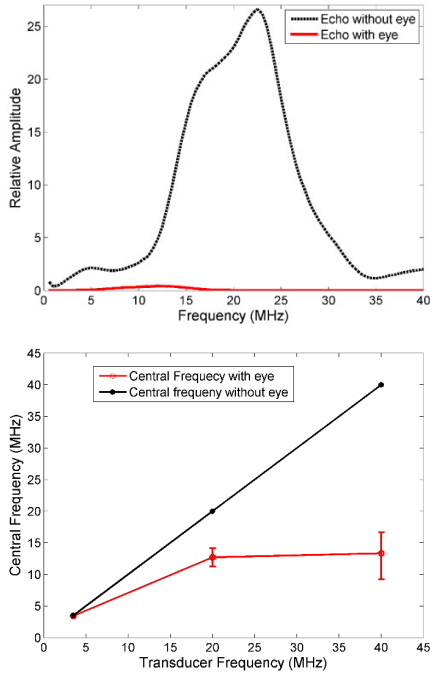

Figure 2: The central frequency shift after ultrasound penetration through porcine eyes. (a) Spectrum of the 3.5-MHz focused transducer; (b) Spectrum of the 20-MHz focused transducer; (c) Central frequency shift.

Simulation studies were carried out to help explain the center frequency shift. Ideally, a three-dimensional (3D) time-domain numerical simulation of wave propagation through the eyeball should be conducted to mimic the experimental conditions. This is, however, extremely time-consuming, given that the eyeball size is significantly larger than the wavelength at the frequency of interest (e.g., 20-MHz). As an alternative, we carried out two-dimensional (2D) frequency-domain simulations using the commercial finite element software COMSOL (COMSOL, Inc., Burlington, MA) to examine the transmission of ultrasound waves through the eyeball. The results can at least qualitatively explain the center frequency shift observed in the experiment.

The simulation setup is shown in Figures 3(a) and (b). Different parts of the eyeball are drawn in different colors. The acoustic parameters used for each layer are collected from references [9,10,28] and listed in Table 2. Perfectly matched layers (PML) were utilized to minimize reflection from the boundary. The PML is an artificial absorbing layer for ultrasonic wave modeling of open boundaries field, in which the reflection wave can be ignored.

A planar transducer with a width of 4mm was simulated at two different frequencies: 10-MHz and 20-MHz. Two different cases (with and without the eyeball) were investigated. Figure 3(c) shows the acoustic pressure profiles along the y-direction, whereas Figure 3(d) illustrates the acoustic pressure profile along the x-direction at approximately 30-mm away from the transducer surface. Two observations can be made: (1) Due to the stronger attenuation at 20-MHz, the 10-MHz pressure magnitude behind the eyeball was about 10- ~ 15-dB higher. When taking into consideration the roundtrip that occurs in the pulse-echo experiment, the pressure magnitude difference between the two frequencies could be as large as 20- ~ 30-dB and contribute to the center frequency shift. (2) Pressure magnitude dramatically reduces as the sound enters the lens (from roughly 6- to 14-mm). This is expected since the lens has the largest attenuation and is mostly responsible for the frequency shift.

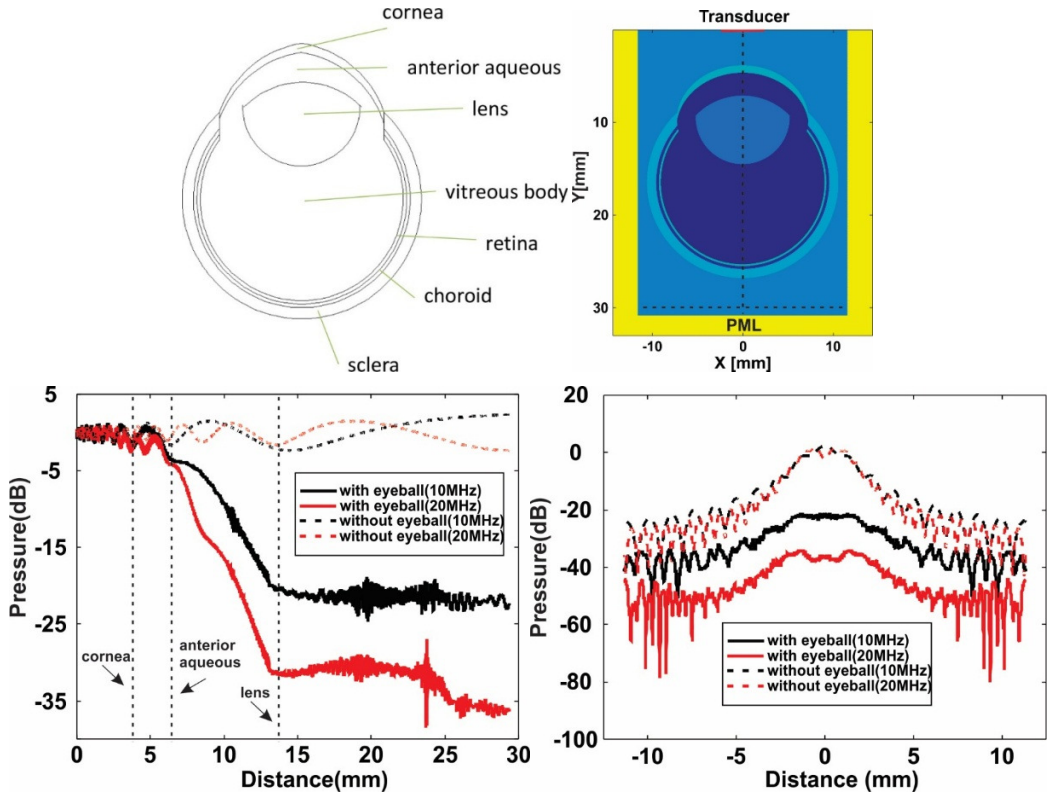

Figure 3: Two-dimensional simulated acoustic pressure profile in multilayered eyes at frequencies of 10-MHz and 20-MHz (a) Sketch of the porcine eye; (b) The structure of the eye for simulation; (c) Pressure profile along - y-direction; (d) Pressure profile along the x-direction.

Layers	Thickness (mm)	Density (g/mm3)	Velocity (mm/s)	β	n	Attenuation (dB/cm)	
						1-MHz	20-MHz
cornea	0.8	0.9445	1587.8	0.0896	1.6788	1.15	13.7
anterior aqueous	2.47	1.0075	1500.7	1.7816	0.0996	0.083	2.4
lens	7.4	1.09	1633.3	4.3675	0.7151	1.33	37.2
retina	0.2	1.03	1548.5	0.041	1.8063	0.83	9.19
choroid	0.3	1.03	1546.8	0.1508	1.6191	1.56	19.27
sclera	1	1.033	1653.8	0.2838	1.466	1.68	22.92
vitreous body	11.83	1.0075	1500.7	1.7816	0.0996	0.083	2.4

Table 2: Parameters of the porcine eye

Attenuation at different frequencies: As described in Eq. (3), the attenuation coefficient will increase as the frequency becomes higher. The measurement result shown in Figure 4 reveals this trend. At the lowest frequency (3.5-MHz), the attenuation coefficient ranges from 0.11-dB/cm to 0.17-dB/cm with an average value of 0.13-dB/cm. At 20-MHz, the attenuation coefficient ranges from 1.03-dB/cm to 1.88-dB/cm with an average value of 1.43-dB/cm. At 40-MHz, the attenuation coefficient ranges from 1.76-dB/cm to 2.42-dB/cm with an average value of 2.15-dB/cm. Assuming the diameter of the pig eye is 24-mm [29], the one-way amplitude attenuation for 3.5-MHz, 20-MHz, and 40-MHz will be 3.12-dB, 34.32-dB, and 51.6-dB, respectively. The intensity loss through the entire eye will be 51.25%, 96.31%, and 99.93%, values which are slightly larger than the modeling result in reference [8]. As a result, relatively high input energy must be used for high-frequency stimulation.

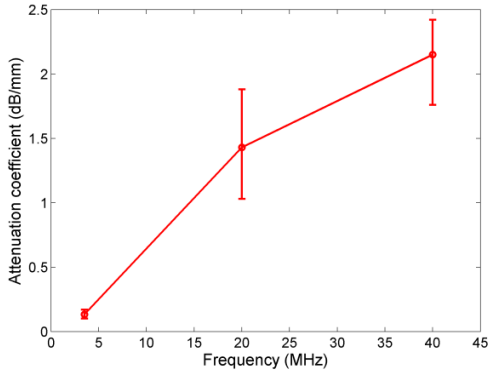

Figure 4: Overall attenuation coefficient at different frequencies

If the thickness and attenuation coefficient of each layer are known, the overall attenuation coefficient of the intact eye can be calculated by dividing the total attenuation by the eye thickness. Previous results on the measured thickness and attenuation coefficient at certain frequencies are provided in Table 2 and are used to calculate the coefficient β and n in formula (3). Then formula (3) can be used to calculate the overall attenuation coefficient at different frequencies. The calculated overall attenuation coefficients are 0.46-dB/cm, 1.47-dB/cm, and 2.41-dB/cm for 3.5-MHz, 20-MHz, and 40-MHz, respectively. The calculated overall attenuation coefficient is very close to the measurement result at 20-MHz. However, the calculated overall attenuation coefficients at the other two frequencies (3.5-MHz and 40-MHz) are larger than the measurement results. The reason may be that the thicknesses listed in Table 2 were measured incorrectly. Therefore, it is necessary to conduct attenuation measurements on the intact eye.

Attenuation of each layer: In order to measure attenuation at the interface of the vitreous body and retina (i.e., epiretinal surface), the sclera, choroid, and retina at the posterior eyeball were removed. A 10-μm thick sheet of parylene, whose attenuation was negligible, was used to cover the hole to prevent the vitreous body from flowing out. The overall attenuation coefficients for the three types of samples we tested are shown in Figure 5. For the intact eye, the coefficients are 1.43-dB/cm and 2.15-dB/cm at frequencies of 20-MHz and 40-MHz respectively, as mentioned above, while the coefficients for the eye without the back are 1.66-dB/cm and 2.23-dB/cm, and the coefficients for the eye with a parylene cover are 1.58-dB/cm and 2.36-dB/cm. Although slight differences are observed, the attenuation coefficient of all three types of samples is within the same error range as shown in Figure 5. The reason may be that the attenuation coefficients of the cut three layers are close to the average value of the intact eye. Therefore, it is acceptable to use the intact eye to estimate the intensity loss instead of using the dissected one.

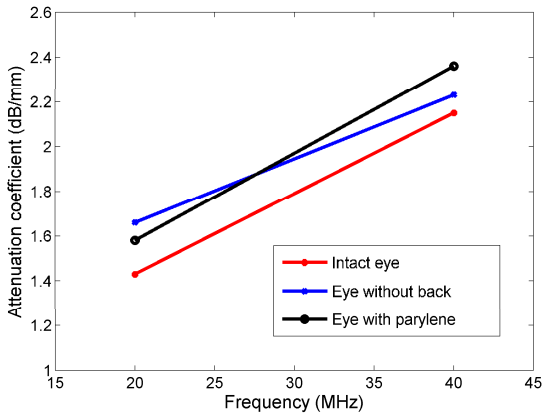

Figure 5: Comparison of the overall attenuation coefficient of different samples

Comparison of focused and planar transducers: The lateral resolution of the focused transducer at a frequency of 40-MHz and with a focal length of 23.5-mm is 220-μm, which is much smaller than that of the planar transducer. The acoustic field emitted by focused and planar transducers in the eyeball is different, but the measured attenuation coefficients are very similar, as shown in Figure 6. This is to be expected since the tissue acoustic parameters depend on the frequency rather than the acoustic field.

The overall attenuation coefficients measured by the focused transducer are 1.44-dB/cm and 2.1-dB/cm at frequencies of 20-MHz and 40-MHz respectively while the values are 1.42-dB/cm and 2.2-dB/cm for the planar transducer. There is no obvious difference between the measurement results from the two types of transducers.

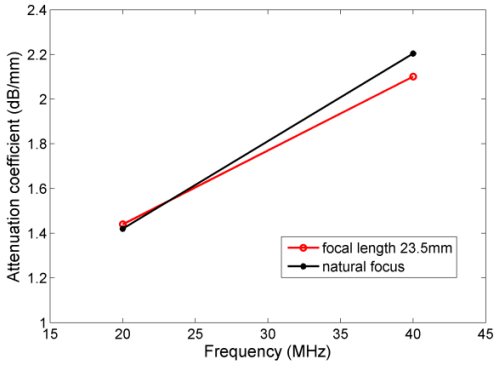

Figure 6: Comparison of overall attenuation coefficient between focal and planar transducers

Conclusion: In this paper, transducers of different frequencies ranging from 3.5-MHz to 40-MHz were used to measure the central frequency shift and attenuation of ultrasound propagation in porcine eyes. The results show that the center frequency of the signal shifted to less than 15-MHz for both 20-MHz and 40-MHz transducers while no significant frequency shift occurred for the 3.5-MHz transducer. These effects are due to the significant attenuation the lens at high frequencies. The overall attenuation coefficients of the porcine eye are 0.13-dB/cm, 1.43-dB/cm, and 2.15-dB/cm at 3.5-MHz, 20-MHz, and 40-MHz respectively, which lead to intensity losses of 51.25%, 96.31%, and 99.93% for an eye with a thickness of 24-mm. The measured attenuation coefficients of intact and dissected eyes are very similar, indicating that no dissection is needed to measure intensity attenuation at the interface of the vitreous body and retina. The attenuation coefficients measured from focused and planar transducers are also similar, implying that the measured data could be used for different types of transducers in future work. The results of this study will be useful for selecting transducers for retinal ultrasonic stimulation. Our findings indicate that transducers with frequency lower than 20-MHz undergo relatively little attenuation. However, the higher frequency (>40-MHz) could provide better axial resolution (26.2-μm) than lower frequency (67.8-μm). So, there is a trade-off between frequency and spatial resolution. Future work may focus on the modeling and measurement of acoustic intensity distribution in the eye for pattern stimulation [4], which has the potential to activate 2D patterns of cells in the retina.

References:

1. Weiland JD, Liu W, Humayun MS (2005) Retinal prosthesis. Annu Rev Biomed Eng 7: 361-401.
2. Ahuja AK, Dorn JD, Caspi A, McMahon MJ, Dagnelie G, et al. (2011) Blind subjects implanted with the Argus II retinal prosthesis are able to improve performance in a spatial-motor task. Br J Ophthalmol 95: 539-543.
3. Garg SJ, Federman J (2013) Optogenetics, visual prosthesis and electrostimulation for retinal dystrophies. Curr Opin Ophthalmol 24: 407-414.
4. Tufail Y, Yoshihiro A, Pati S, Li MM, Tyler WJ (2011) Ultrasonic neuromodulation by brain stimulation with transcranial ultrasound. Nat Protoc 6: 1453-1470.
5. Tufail Y, Matyushov A, Baldwin N, Tauchmann ML, Georges J, et al. (2010) Transcranial pulsed ultrasound stimulates intact brain circuits. Neuron 66: 681-694.
6. Legon W, Sato TF, Opitz A, Mueller J, Barbour A, et al. (2014) Transcranial focused ultrasound modulates the activity of primary somatosensory cortex in humans. Nat Neurosci 17: 322-329.
7. Naor O, Hertzberg Y, Zemel E, Kimmel E, Shoham S. (2012)Towards multifocal ultrasonic neural stimulation II: design considerations for an acoustic retinal prosthesis. J Neural Eng 9: 026006.
8. Menz MD, Oralkan O, Khuri-Yakub PT, Baccus SA (2013) Precise neural stimulation in the retina using focused ultrasound. J Neurosci 33: 4550-4560.
9. Chivers RC, Round WH, Zieniuk JK (1984) Investigation of ultrasound axially traversing the human eye. Ultrasound Med Biol 10: 173-188.
10. De Korte CL, van der Steen AFW, Thijssen JM (1994) Acoustic velocity and attenuation of eye tissues at 20 MHz. Ultrasound Med Biol 20: 471-480.
11. Ye SG, Harasiewicz KA, Pavlin CJ, Foster FS (1995) Ultrasound characterization of normal ocular tissue in the frequency range from 50 MHz to 100 MHz. IEEE Trans Ultrason Ferroelectr Freq Control. 42: 8-14.

12. Huang CC, Ameri H, Deboer C, Rowley AP, Xu X, et al. (2007) Evaluation of lens hardness in cataract surgery using high-frequency ultrasonic parameters in vitro. Ultrasound Med Biol 33: 1609-1616.
13. Huang CC, Zhou Q, Ameri H, Wu DW, Sun L, et al. (2007) Determining the acoustic properties of the lens using a high-frequency ultrasonic needle transducer. Ultrasound Med Biol 33: 1971-1977.
14. Coleman DJ, Daly SW, Atencio A, Lloyd HO, Silverman RH (2009) Ultrasonic Evaluation of the Vitreous and Retina. Semin Ophthalmol 13: 210-218.
15. Huang CC, Chen R, Tsui PH, Zhou Q, Humayun MS, et al. (2009) Measurements of attenuation coefficient for evaluating the hardness of a cataract lens by a high-frequency ultrasonic needle transducer. Phys Med Biol 54: 5981-5994.
16. Caixinha M, Jesus DA, Velte E, Santos MJ, Santos JB (2014) Using ultrasound backscattering signals and Nakagami statistical distribution to assess regional cataract hardness. IEEE Trans Biomed Eng 61: 2921-2929.
17. Coleman DJ, Silverman RH, Chabi A, Rondeau MJ, Shung KK, et al. (2004) High-resolution ultrasonic imaging of the posterior segment. Ophthalmology 111: 1344-1351.
18. Williams DL, Goddard PJ, Brancker WM (2007) Ultrasonographic examination of ocular lesions in farmed halibut. Vet J 173: 456-458.
19. Silverman RH, Ketterling JA, Mamou J, Coleman DJ (2008) Improved high-resolution ultrasonic imaging of the eye. Arch Ophthalmol 126: 94-97.
20. Kim HH, Hu C-H, Park J, Kang BJ, Williams JA, et al. (2010) Characterization and evaluation of high frequency convex array transducers. Ultrasonics Symposium (IUS), IEEE.
21. Cha JH, Chang JH (2014) Development of 15MHz 2-2 piezo-composite ultrasound linear array transducers for ophthalmic imaging. Sensor Actuat A-phys 217: 39-48.
22. Zhou Q, Lam KH, Zheng H, Qiu W, Shung KK (2014) Piezoelectric single crystals for ultrasonic transducers in biomedical applications. Prog Mater Sci 66: 87-111.
23. Zhou Q, Xu X, Gottlieb EJ, Sun L, Cannata JM, et al. (2007) PMN-PT single crystal, high-frequency ultrasonic needle transducers for pulsed-wave Doppler application. IEEE Trans Ultrason Ferroelectr Freq Control 54: 668-675.
24. Shung KK (2009) High frequency ultrasonic imaging JMU 17: 25-30.
25. Cannata JM, Williams JA, Zhang L, Hu CH, Shung KK (2011) A high-frequency linear ultrasonic array utilizing an interdigitally bonded 2-2 piezo-composite. IEEE Trans Ultrason Ferroelectr Freq Control 58: 2202-2212.
26. Hsu HS, Zheng F, Li Y, Lee C, Zhou Q, et al. (2012) Focused high frequency needle transducer for ultrasonic imaging and trapping. Appl Phys Lett 101: 24105.
27. Shung KK (2015) Diagnostic ultrasound: Imaging and blood flow measurements, Second Edition. CRC press 291.
28. Sanchez I, Martin R, Ussa F, Fernandez-Bueno I (2011) The parameters of the porcine eyeball. Graefes Arch Clin Exp Ophthalmol 249: 475-482.
29. Bertschinger DR, Beknazar E, Simonutti M, Safran AB, Sahel JA, et al. (2008) A review of in vivo animal studies in retinal prosthesis research. Graefes Arch Clin Exp Ophthalmol 246: 1505-1517.

Acknowledgements: This work was supported in part by the National Institutes of Health under grants 1R01EY026091 and P41 EB2182 and RPB